

State-of-the-Art Image Motion Deblurring Technique

Hang Qiu
5090309140
Shanghai Jiao Tong University
qhqd0708sl@gmail.com

Abstract

In this paper, image motion deblurring technique is widely surveyed and discussed. We compare and contrast some of the most recent literature in this field by introducing both their methodology and approach and their deblurring result of synthetic and real image. Throughout the analysis, we bring out some state-of-the-art approach and further discuss possible future work and direction..

1. Introduction

Image motion blur is the vague phenomenon happened on the obtained picture when the sensor is moving during the exposure or it is exposed at several different places. In recent literature, image motion blur is commonly modeled as the convolution between a sharp clear image and a blur kernel:

$$y = k \otimes x \quad (1)$$

where x is latent sharp image, k representing the blur kernel and y the obtained blurry image. The \otimes indicates the convolution operation. As the topic is researched, more and more problems have been considered such as uniform and non-uniform blur, different depth-layer, etc. And multiple method has been proposed such as classic MAP algorithm with various supplementary priors and estimators.

In this paper, we will list and analyze those most recent literature on motion deblurring, introducing their methodology and approach, and comparing their deblurring result with both synthetic and real image. Throughout the analysis, we bring out some state-of-the-art approach and further discuss possible future work and direction..

The following part of this paper will be arranged like this: first we include almost all the recent works and literature in section 2. Then in section 3 and section 4, we will compare and contrast some of the most recent techniques by introducing both their methodology and approach and their deblurring result of synthetic and real image. Finally, we will discuss possible future work and direction in section 5

2. Related Work

Most recent image motion deblurring technique can be categorized into two basic classes: Singla Image Deblurring and Multi-image Deblurring. Based on the fundamental assumptions of blurring process, they can be further distinguished into spatially invariant point spread function (PSF) estimation and spatially variant PSF estimation.

In single image deblurring, Fergus *et al.* [1] proposed a variational Bayesian approach to estimate the blur kernel by maximizing the marginal probability. Levin *et al.* [2] proposed an improved efficient marginal likelihood approximation. Detailed analysis of the MAP problem in motion deblurring was provided in [3]. Several methods [7], [8], [11], [12], [4] followed the line of altering the traditional MAP framework to estimate the blur kernel and latent image iteratively, introducing a two phase (blur kernel and latent image) estimation. In those semi-blind or non-blind deconvolution in each phase, they do not favor the trivial delta kernel and sharp image solution by either explicitly reweighting strong edges [7], predicting sharp edges using different priors [8], [11], [12], [4], [14] or directly imposing normalized sparsity measures on image gradients [13]. The gradient sparsity prior was earlier used by a lot of work including Levin *et al.* [4], calculating Iteratively Re-weighted Least Squares (IRLS) to regularize results for images exhibiting defocus blur and motion blurred images. Krishnan *et al.* [13] analyze all the present priors and introduce an novel sharp-favorite prior for deconvolution. Also, variable substitution schemes [14] were employed to constrain the deconvolution solution. As for detail recovery, Yuan *et al.* [25] proposed a multiscale approach to progressively recover blurred details while Shan *et al.* [7] introduced regularization based on high order partial derivatives to reduce image artifacts. Meanwhile, Raskar *et al.* [31] coded the exposure to make the PSF more suitable for deconvolution. Jia [26] demonstrated how to use an objects alpha matte to better compute the PSF. However, all these methods above assume that the blur kernel is spatially invariant.

Due to the deconvolution problem is severely ill-posed, more information is in need and multi-image methods were

proposed in a lot of literature. Ben-Ezra and Nayar [33] attached a video camera to a conventional highresolution still camera to facilitate PSF estimation. The hybrid camera system was extended by Tai *et al.* [15] to compute general motion blur with optical flow. Li *et al.* [17] developed a three-camera system to remove object motion blur and restore scene depth. In [18], Yuan *et al.* took an additional noisy-unblurred image to form a noisy/blurred image pair, making PSF estimation robust. Two blurred images were also used in [19] for motion deblurring. Assuming constant velocity camera motion, Li *et al.*[20] used a set of motion-blurred frames to create a deblurred panoramic image.

All these single-image and multi-image methods do not consider the fact that many scenes comprise multiple depth layers, which cause abrupt PSF change in different image layer. Actually, real camera shake does not in general cause uniform blur [3]. A natural thought is to segment an image into multiple regions, each with a constant PSF as demonstrated by Levin [6], Bardsley *et al.* [32], Cho *et al.* [9] and Li *et al.* [17]. Such segmented regions, however, should be small to make the constant PSF assumption valid for the spatially varying motion blur in camera shake motion. For example, Tai *et al.* [15],[16] extended the hybrid camera framework used by Ben-Ezra and Nayar [33] to estimate a PSF per pixel using an auxiliary video camera. This need for a per-pixel PSF revealed the futility of relying on the conventional kernel based PSF model for spatially varying blur due to ego motion. Meanwhile, Joshi *et al.*[21] proposed a hardware solution with motion inertia sensors to estimate camera shake. Simplified rotation model, motion density function (MDF) model and forward model were introduced in [22],[24] and [23] to handle non-uniform blur. The work presented in [26],[28],[29], on the other hand, focused on partial detection or removal of blur caused by object motion. For the most recent work, Cho *et al.* (2011) [10] explicitly handles outliers based on the deconvolution process, while Jia *et al.* (2012)[27] deal with depth-variation-involved motion deblurring using prevailing stereo cameras.

3. Spatially Invariant Deblurring

Spatially invariant delurring is based on a fundamental assumption that the blur kernel of an observed image is uniform. As the kernel is unknown from an input blurred image, this assumption could largely simplify the solution of the deblurring process. Blind deconvolution is the most common way of recovering a sharp version of an input blurry image when the blur kernel is unknown. Numerous papers in the signal and image processing literature have done a lot research on this subject. Earlier work can be found in the survey in 1996 [34].Recent algorithms have proposed to address the ill-posedness of blind deconvolution by characterizing latent image using natural image statistics. Although the assumption is far from reality, recent deblurring

approach is still encouraging.

In this section, we will first analyze the standard MAP algorithm and its failure, and bring out other modification method. Finally we will evaluate those methods by comparing their deblurring results using common dataset.

3.1. MAP algorithm and its failure

The standard MAP algorithm has been researched widely and deeply analyzed by Levin *et al.* in 2009 [3] and krishnan in 2011 [13]. The common assumption of a blurred image y is as in equation 2.

$$y = k \otimes x + n \quad (2)$$

where x is latent sharp image and k is blur kernel, n representing the noise (common assumption is *i.i.d* Gaussian noise). The simplest approach is a maximum-a-posteriori($MAP_{x,k}$) estimation, seeking a pair (x,k) maximizing:

$$p(x, k|y) \propto p(y|x, k)p(x)p(k) \quad (3)$$

where $p(y|x, k)$ is likelihood term, usually representing the data fitting term $\log p(y|x, k) = -\lambda||k \otimes x - y||^2$. The prior $p(x)$ favors natural images, usually based on the observation that their gradient distribution is sparse. A common measure is

$$\log p(x) = - \sum_i |g_{x,i}(x)|^\alpha + |g_{y,i}(x)|^\alpha + C \quad (4)$$

where $g_{x,i}(x)$ and $g_{y,i}(x)$ denote the horizontal and vertical derivatives at pixel i and C is a constant normalization term. Exponent values $\alpha < 1$ lead to sparse priors and natural images usually correspond to α in the range of [0.5, 0.8]. Other choices include a Laplacian prior $\alpha = 1$, and a Gaussian prior $\alpha = 2$.

If we use the common measure in Eq.4 as an example, the whole optimization problem is

$$(x, k) = \arg \min_{x, k} \lambda ||k \otimes x - y||^2 + \sum_i |g_{x,i}(x)|^\alpha + |g_{y,i}(x)|^\alpha \quad (5)$$

As is claimed and proved by Levin *et al.* in [3],the pair (x, k) optimizing the $MAP_{x,k}$ problem satisfies $|x| \rightarrow 0$ and $|k| \rightarrow \infty$.That is to say the most likely image under the prior in Eq.5 is a flat image with no gradients. One attempt to fix the problem is to assume the mean intensity of the blurred and sharp images should be equal, and constrain the sum of k : $\sum_i k_i = 1$. This eliminates the zero solution, but it still favors the no-blur solution.

3.2. Extension and Modification on MAP algorithm

3.2.1 Priors

After Fergus *et al.* [1] introduced the basic MAP model in Eq.3 , numerous modification [7, 8, 11, 26, 9, 12, 28]

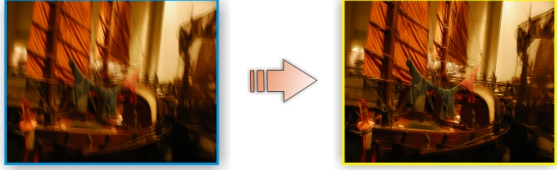


Figure 1. Deblurring Result of [7]

of MAP algorithm has been proposed. On more advanced priors, [24, 4, 5] use L_p -norms on the gradients, with $p \in [0.7, 1]$, reflecting the statistics of natural images. To handle the spatial randomness in noise, Shan *et al.* [7] propose the likelihood prior to be

$$p(y|x, k) = \prod_{\partial^* \in \theta} \prod_i N(\partial^* y_i | \partial^* y_i^c, \delta_{\kappa(\partial^*)}) \quad (6)$$

where y^c is the reconvolved image $y^c = k \otimes x$. They only use the first two order derivatives $\theta = \{\partial^0, \partial_x, \partial_y, \partial_{xx}, \partial_{xy}, \partial_{yy}\}$. As for blur kernel sparse prior, they use the common exponentially distributed prior

$$p(k) = \prod_j e^{-\tau x_j} \quad (7)$$

As for latent image prior, they approximated the distribution of natural image logarithmic gradient (shown in Fig. ??)

$$\phi(x) = \begin{cases} -k|x| & x \leq l_t \\ -(ax^2 + b) & x > l_t \end{cases} \quad (8)$$

and introduce a global prior $p_g(x)$ and local prior $p_l(x)$ to both reduce the ill-posedness and the ringing artifacts.

$$p(x) = p_g(x)p_l(x) \quad (9)$$

$$p_g(x) \propto \prod_i e^{\phi(\partial x_i)} \quad (10)$$

$$p_l(x) = \prod_{i \in \omega} N(\partial_x x_i - \partial_x y_i | 0, \sigma_1) N(\partial_y x_i - \partial_y y_i | 0, \sigma_1) \quad (11)$$

The deblurring result is shown in Fig.1.

Based on the analysis of Levin [3], one key property making blind deconvolution possible is the strong asymmetry between the dimensionalities of x and k . While the number of unknowns in x increases with image size, the dimensionality of k remains small. Although the larger-scale object can yield stable kernel estimation because it is wider than the kernel, preserving the total variation of the latent

signal along its edges, a blurred image with rich edge information along many small-scale objects may not yield accurate stable kernel. The correct kernel estimate cannot be found, primarily due to the small structure problem. So, using a similar two phase iterative algorithm, Jia *et al.* [12] propose a new criterion for selecting informative edges for kernel estimation. The criterion measure the usefulness of gradients as follows

$$r(x) = \frac{\|\sum_{i \in W_h(x)} \nabla y(i)\|}{\sum_{i \in W_h(x)} \|\nabla y(i)\| + 0.5} \quad (12)$$

where $W_h(x)$ is a $h \times h$ window centered at pixel x . 0.5 is to prevent producing a large r in flat regions. The deblurring result, together with results of [8, 13] are shown and compared in Fig.2.

As noted by krishnan *et al.* [13], Levin *et al.* [3] and Fergus *et al.*[1], somewhat counterintuitively, the priors all favor blurry images to sharp images. In other words, blurry images have lower cost (are more probable) than sharp images. This is a direct result of the learned/chosen potential functions decreasing toward zero: since blur attenuates high frequencies, the response of any derivative-type filter will also be reduced and consequently will have a lower cost under the model. Taking widely used L_1 -norm as an example, In an image setting, the L_1 norm is typically used to penalize the high frequency bands. As image noise presents itself in these bands, boosting their L_1 norm, minimizing the norm is a way of denoising the image. However, in the case of image blur, the opposite situation holds since blur attenuates the high frequency bands so reducing their L_1 norm. Thus, minimizing the L_1 norm on the high frequencies of the image will result in a blurry image.

In 2011, krishnan *et al.* [13] proposed a novel prior using the ratio of L_1 -norms and L_2 -norms, which favors no-blur explanation as illustrated in Fig.?? .The optimization problem is formed like

$$(x, k) = \arg \min_{x, k} \lambda \|k \otimes x - y\|^2 + \frac{\|x\|_1}{\|x\|_2} + \phi \|k\|_1 \quad (13)$$

Similarly, the equation subject to the constraint that $k \geq 0, \sum_i k_i = 1$, and the problem is solved two-phase iteratively.

The $L_1 L_2$ norms function does have several drawbacks. First, it is non-convex, unlike L_1 norms , thus there are multiple localminima. Finally, it cannot be expressed as a probabilistic prior. This is in direct contrast to l_p norms ($0.7 \leq p \leq 1$) which correspond to probabilistic models of image gradients, having a (hyper)-Laplacian form [14]. It is only suitable for a non-probabilistic framework.



Figure 2. Spatially Invariant Deblurring Result Comparison I. From left to right: a) Blurry input image.b)Cho *et al.* [8] (2009). c) Jia *et al.* [12] (2010). d) Krishnan *et al.* [13] (2011).

3.2.2 Two Phase Iterative Approach

Due to the same small structure problem aforementioned, while a simultaneous MAP estimation of both x and k fails, a MAP estimation of k alone (marginalizing over x), is well constrained and recovers an accurate kernel[1, 2]. That is also why two phase iterative method comes in. Although the sparse priors mentioned in former sections are helpful, the key component making blind deconvolution possible is not the choice of prior, but the thoughtful choice of estimator.Two phase approach normally use a MAP_k estimator to recover the kernel and, given the kernel, solve for latent image x using a non-blind deconvolution algorithm. For classic non-blind deconvolution, we refer the readers to the comprehensive survey [35] for more details.In this section, we focus on some of most recent work and explain their iterative approach to solve the ill-posed problem.

To start with, Shan *et al.*(2008) [7], based on the priors introduced earlier, transform the MAP problem into an energy minimization problem:

$$E(x, k) = -\log p(x, k|y) \\ \propto \left(\sum_{\partial^* \in \theta} \omega_{\kappa(\partial^*)} \|\partial^* x \otimes k - \partial^* y\|_2^2 + \lambda_1 \|\phi(\partial_x x) + \phi(\partial_y x)\|_1 + \lambda_2 (\|\partial_x x - \partial_x y\|_2^2 + \|\partial_y x - \partial_y y\|_2^2) + \|k\|_1 \right) \quad (14)$$

where the first term is the likelihood term, the second and third is about the matching condition with latent image and blurred image, the last being the kernel term. When optimizing latent image x , just ignore the last term, and when optimizing blur kernel, ignore the second and third term.

To improve the speed, Cho *et al.* (2009) [8] simplified Eq.14. When estimating the image:

$$E(x) = \sum_{\partial^* \in \theta} \omega_{\kappa(\partial^*)} \|\partial^* x \otimes k - \partial^* y\|_2^2 + \alpha \|\nabla x\|_2^2 \quad (15)$$

When estimating the kernel:

$$E(k) = \sum_{\partial^* \in \theta} \omega_{\kappa(\partial^*)} \|\partial^* x \otimes k - \partial^* y\|_2^2 + \beta \|k\|_2^2 \quad (16)$$



Figure 3. Deblurring Result of [8]

Still, Cho only use θ as upto the second order derivatives. One thing worth to be mentioned is that, since their method uses only image derivatives, it can avoid the boundary artifacts by simply padding the boundaries of the derivative images. By setting the width of a padded image as a power of prime numbers, 2, 3, 5, and 7, which is greater than or equal to $(n + m - 1)$, where n and m are the widths of the input image and the kernel, respectively. The height of a padded image is determined similarly. Thus, FFTs can be computed quickly for such image sizes.Their deblurring result can be seen in Fig. 3

Similarly, Jia *et al.* (2010) [12] and krishnan *et al.*(2011) [13] applied their own unique spatial prior and L_1L_2 prior to the same two phase iteration scheme. For instance, in [13], the two phase energy representation becomes:

$$E(x) = \lambda \|k \otimes x - y\|^2 + \frac{\|x\|_1}{\|x\|_2} \quad (17)$$

$$E(k) = \lambda \|k \otimes x - y\|^2 + \phi \|k\|_1 \quad (18)$$

Levin *et al.* (2011) [2], improving the marginalized approach proposed by Fergus *et al.*[1], introduced the covariance into the current latent image estimation phase, They derived this simple algorithm by casting the MAP_k problem in the Expectation-Minimization framework where the latent variable is the sharp image x .

As mentioned in Section 2, multi-image deblurring has also been deeply researched. For instance, Yuan *et al.* [18] use noisy/blurred image pairs to make a robust PSF estimation. During their multi-image kernel and latent image estimation, they apply two phase approach as well. Specifically, in kernel estimation, they use Landweber method to iteratively solve Eq. 16. And they introduce a residual deconvolution and gain-controlled Richardson-Lucy (RL) algorithm to further suppress ringing artifact.



Figure 4. Spatially Invariant Deblurring Result Comparison II. From left to right: a) Blurry input image.b)Yuan *et al.* [18] (2007). c) Shan *et al.* [7] (2008). d) Cho *et al.* [8](2009).

Most of the optimization problem mentioned above is solved by using a conjugate gradient (CG) approach, normally within 10 iteration. Some of them, like [2] and [8], apply multiscale approach or a coarse-to-fine scheme, using bilateral interpolation in upsampling the kernel, to further improve the performance on both small and large blurs.

3.3. Evaluation and Comparison

In this section, we will choose some of the deblurring result of spatially invariant blurry image which are deblurred by using those most recent technique introduced in the literature mentioned in section 3.2 and section 3.2.2, to compare and contrast different approach.

Shown in Fig.4, we can see that although the estimated kernel are different from each other, the deblurring result are all encouraging despite of some little ringing artifact which can still be observed carefully. While yielding similar result, Yuan *et al.* [18] used two images, Shan *et al.* [7] used only one image and Cho *et al.* [8] approach are much more efficient and less time consuming.

As is shown in Fig. 2, [8, 12, 13] all use a two phase iterative approach. Although they adopt different priors, the result yeilded similar. With comparison of speed, [8] is still faster than the other two, while [13] yeild a relatively better result with a tolerate speed.

4. Spatially Variant Deblurring and Further Discussion

In contrast with spatially invariant deblurring, spatially variant deblurring assumes a non-uniform blur which is more realistic. As is shown section 3, most of of existing blind deconvolution research concentrates at recovering a single blurring kernel for the entire image. However, in the case of different motions, the blur cannot be modeled with a single kernel, and trying to deconvolve the entire image with the same kernel will cause serious artifacts. Thus, the focus here is how to model or describe the different blur and numerous approach on spatially variant deblurring has been proposed.

To start with, Levin *et al.*(2006) [6] analyze the statistics of derivative filters in images are significantly changed by blur. And by assuming the blur results from a constant velocity motion, they can limit the search to one dimensional box filter blurs. They model the expected derivatives distributions as a function of the width of the blur kernel, by which they use to powerfully discriminate regions with different blurs.

They then define the log-likelihood of the derivatives in a window with respect to each of the blurring models to measure how well the i'th window is explained by a k-tap blur.

$$l_k(i) = \sum_{j \in W_i} \log p_k(\partial_x x(j)) \quad (19)$$

where W_i is a window around pixel i and p_k is the distribution of horizontal derivatives after blurred by a k-tap kernel.

Then they segment the different blur region smoothly by maximizing the likelihood of derivative in each region, which is transformed into minimizing the energy function:

$$E(k) = \sum_i -l_k(x(i, i)) + \sum_{\langle ij \rangle} e_{ij} |x(i) - x(j)| \quad (20)$$

where e_{ij} is the smooth term:

$$e_{ij} = \lambda + v(|x(i) - y(i)| + |x(j) - y(j)|) \quad (21)$$

The smoothness term is combined from two parts. The first is just a constant penalty for assigning different labels to neighboring pixels, thus preferring smooth segmentations. The second part encodes the fact that it is cheaper to cut the image in places where there is no visual seam between the original and the deconvolved images.

Meanwhile, in terms of rotational blur, Whyte *et al.* (2010) [22] propose a new parametrized geometric model of the blurring process in terms of the rotational velocity of the camera during exposure. This model can be applied either on single image blind deblurring and blurry/noisy-pairs image deblurring.

Furthermore, Gupta *et al.* (2010) [24]introduce the motion density function (MDF),which records the fraction of

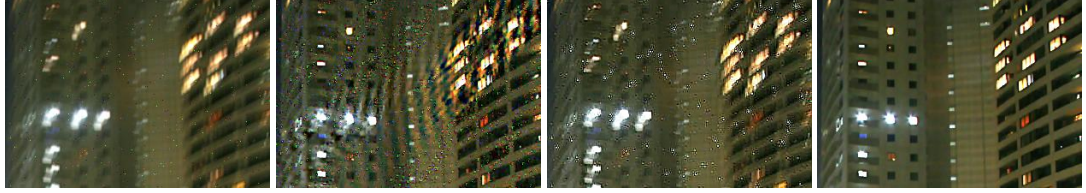


Figure 6. Outliers Deblurring Comparison. Left: Blurry input image. Middle left: Levin *et al.* [5] (2007). Middle right: Jia *et al.* [27] (2012). Right: Cho *et al.* [10] (2011)

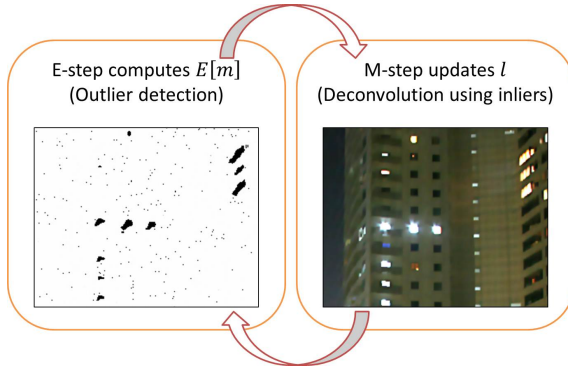


Figure 5. Handling Outliers [10]

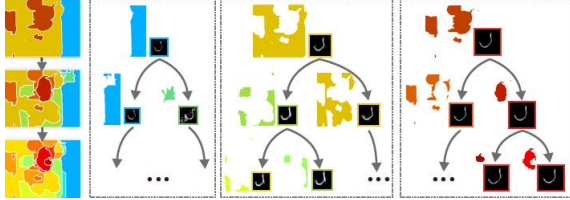


Figure 7. Region-tree Segmentation of [27]

time spent in each discretized portion of the space of all possible camera poses, to describe the spatially varying blur kernels. They decomposed the blur kernel into different sub-kernels:

$$k = \sum_j \alpha_j k_j \quad (22)$$

Thus, similar to blind deconvolution with a sparse prior $\phi()$ as well, they form the energy minimization like:

$$\begin{aligned} E(x, k) = & \left\| \left(\sum_j \alpha_j k_j \right) \otimes x - y \right\|_2^2 + \\ & \|\phi(|\partial_x x|) + \phi(|\partial_y x|) + \lambda_1 \|A\|^\gamma + \lambda_2 \|\nabla A\|^2 \end{aligned} \quad (23)$$

where A is the MDF matrix where each element α_j denotes the density at the camera pose j . The deblurring result is shown as in Fig. 8. Though variant MDF can solve some non-uniform problem, it is still outperformed by depth-aware deblurring in Top right.

Similarly, in terms of handling the non-linearity of blur kernel, instead of model them as different sub-kernels, Cho *et al.* (2011) [10] modeled them as outliers of the linear deconvolution function, and explicitly handles them in the deconvolution process. Note that by outliers, we mean the saturated pixel and non-Gaussian noise which may yield artifact in the deconvolution process due to the contradiction to the deconvolution assumption. The outliers handling process is shown in Fig.5. This unique method in comparison with some other spatially variant deblurring method is shown in Fig.6. As we can see, for the saturated pixel, even the newest technique from Jia *et al.* cannot handle it properly while specifically designed method [10] can restore the image well. That is to say, different technique is sometimes particularly suitable for certain images while it may fail on other challenging ones.

For the most recent work, Jia *et al.* (2012) [27] noted that existing non-uniform deblurring methods cannot handle image with different depth layer, because when objects are not far from the camera, spatially-varying point-spread-functions (PSFs) arise along with abrupt change along the boundaries, making a near point be blurred more than a distant one. As we can see smooth kernel change is no longer applicable at the edge of different depth objects. So they apply two image to use a two-view stereo analysis to form a depth-aware blur kernel to handle this situation. The two-view analysis is based on:

$$I_m(x) = I_r(x + \frac{f}{z(x)} \delta b) = I_r(x + d_m(x)) \quad (24)$$

where I_m is unblurred matching image and I_r is the reference image, δb is the baseline distance between the two camera projection centers, $z(x)$ denotes the depth of x in the matching view, and $d_m(x)$ is the disparity of the point that projects to x in I_m . According to Eq.24, they model different depth layer into different blur sub-kernel like Eq.22 and introduce a region-tree segmentation method shown in Fig.7.

5. Conclusion and Future Work

Through a wide range survey, the most recent deblurring technique includes spatially invariant single image and



Figure 8. Spatially Variant Deblurring Result Comparison I.Left:Blurry input image.Middle:Gupta *et al.* [24] (2010).Right: Jia *et al.* [27] (2012).



Figure 9. Spatially Variant Deblurring Result Comparison II.Left: Blurry input image. Middle: Whyte *et al.* [22] (2010). Right: Jia *et al.* [27] (2012).

multi-image deblurring, spatially variant single image and multi-image deblurring. After evaluation and comparison of the most recent work, as is mentioned earlier, we found that different approach is designed unique and may sometimes especially suitable for some certain images while performing badly on others. Considering the deblurring result of some challenging image such as some with non-uniform blur, the room for improvement is still large. In order to enhance the performance, handle more sophisticated problem like sharp changes of PSF at the edge of different depth-layer, more information may be inevitably needed. However, to yield better performance with fast speed and less information or even only one image is still possible and should be encouraged to research.

References

- [1] R. Fergus, B. Singh, A. Hertzmann, S. T. Roweis, and W. T. Freeman. Removing camera shake from a single photograph. ACM Trans. Graph., 25(3), 2006.
- [2] A. Levin, Y. Weiss, F. Durand, and W. T. Freeman. Efficient marginal likelihood optimization in blind deconvolution. In CVPR, 2011.
- [3] A. Levin, Y. Weiss, F. Durand, and W. T. Freeman. Understanding and evaluating blind deconvolution algorithms. In CVPR, 2009.
- [4] A. Levin, R. Fergus, F. Durand, and W. T. Freeman. Image and depth from a conventional camera with a coded aperture. ACM Trans. Graph., 26(3), 2007.
- [5] A. Levin and Y. Weiss. User assisted separation of reflections from a single image using a sparsity prior. PAMI, 29(9):1647-1654, Sept 2007.
- [6] A. Levin. Blind motion deblurring using image statistics. In NIPS, 2006.
- [7] Q. Shan, J. Jia, and A. Agarwala. High-quality motion deblurring from a single image. ACM Trans. Graph., 27(3), 2008.

- [8] S. Cho and S. Lee. Fast motion deblurring. *ACM Trans. Graph.*, 28(5), 2009.
- [9] S. Cho, Y. Matsushita, and S. Lee. Removing non-uniform motion blur from image. In *ICCV*, 2007.
- [10] S. Cho, J. Wang, S. Lee. Handling Outliers in Non-Blind Image Deconvolution. In *ICCV*, 2011.
- [11] N. Joshi, R. Szeliski, and D. J. Kriegman. Psf estimation using sharp edge prediction. In *CVPR*, 2008.
- [12] L. Xu and J. Jia. Two-phase kernel estimation for robust motion deblurring. In *ECCV* (1), 2010.
- [13] D. Krishnan, T. Tay, and R. Fergus. Blind deconvolution using a normalized sparsity measure. In *CVPR*, 2011.
- [14] D. Krishnan and R. Fergus. Fast image deconvolution using hyper-laplacian priors. In *NIPS*, 2009.
- [15] Y.-W. Tai, H. Du, M. S. Brown, and S. Lin. Image/video deblurring using a hybrid camera. In *CVPR*, 2008.
- [16] Y.-W. Tai, P. Tan, and M. S. Brown. Richardson-lucy deblurring for scenes under a projective motion path. *PAMI*, 33(8), 2011.
- [17] F. Li, J. Yu, and J. Chai. A hybrid camera for motion deblurring and depth map super-resolution. In *CVPR*, 2008.
- [18] L. Yuan, J. Sun, L. Quan, and H.-Y. Shum. Image deblurring with blurred/noisy image pairs. *ACM Trans. Graph.*, 26(3), 2007.
- [19] A. Rav-Acha and S. Peleg. Two motion-blurred images are better than one. *Pattern Recognition Letters*, 26(3), 2005.
- [20] Y. Li, S. B. Kang, N. Joshi, S. Seitz, and D. Huttenlocher. Generating sharp panoramas from motion-blurred videos. In *CVPR*, 2010.
- [21] N. Joshi, S. B. Kang, C. L. Zitnick, and R. Szeliski. Image deblurring using inertial measurement sensors. *ACM Trans. Graph.*, 29(4), 2010.
- [22] O. Whyte, J. Sivic, A. Zisserman, and J. Ponce. Non-uniform deblurring for shaken images. In *CVPR*, 2010.
- [23] O. Whyte1, J. Sivic1, A. Zisserman. Deblurring Shaken and Partially Saturated Images, 2011
- [24] A. Gupta, N. Joshi, C. L. Zitnick, M. F. Cohen, and B. Curless. Single image deblurring using motion density functions. In *ECCV* (1), 2010.
- [25] L. Yuan, J. Sun, L. Quan, and H.-Y. Shum. Progressive interscale and intra-scale non-blind image deconvolution. *ACM Trans. Graph.*, 27(3), 2008.
- [26] J. Jia. Single image motion deblurring using transparency. In *CVPR*, 2007.
- [27] L. Xu, J. Jia. Depth-Aware Motion Deblurring. In *ICCP*, 2012.
- [28] Q. Shan, W. Xiong, and J. Jia. Rotational motion deblurring of a rigid object from a single image. In *ICCV*, 2007.
- [29] A. Chakrabarti, T. Zickler, and W. T. Freeman. Analyzing spatially-varying blur. In *CVPR*, 2010.
- [30] J. Money and S. Kang. Total variation minimizing blind deconvolution with shock filter reference. In *Image and Vision Computing*, number 2, pages 302-314, 2008.
- [31] A. Agrawal and R. Raskar. Resolving objects at higher resolution from a single motion-blurred image. In *CVPR*, 2007.
- [32] J. Bardsley, S. Jefferies, J. Nagy, and R. Plemmons. Blind iterative restoration of images with spatially-varying blur. In *Optics Express*, pages 17671-1782, 2006.
- [33] M. Ben-Ezra and S. Nayar. Motion-based Motion Deblurring. *IEEE Trans. PAMI*, 26(6):689-698, Jun 2004.
- [34] D. Kundur and D. Hatzinakos. Blind image deconvolution. *IEEE Signal Processing Magazine*, 1996.
- [35] M. R. Banham and A. K. Katsaggelos. Digital image restoration. *Signal Processing Magazine*, IEEE, 14(2):24-41, Mar. 1997.